

*To be published in Journal of the Optical Society of America B:*

**Title:** Theoretical investigation of waveguide power splitters with parallel output ports in two-dimensional square lattice photonic crystals

**Authors:** Jianhong Zhou, Chang Qing, Mu Da, Yang Jinhua, Han Wenbo, and Wang Lu

**Accepted:** 27 October 2009

**Posted:** 3 November 2009

**Doc. ID:** 117160

# **Theoretical investigation of waveguide power splitters with parallel output ports in two-dimensional square lattice photonic crystals**

Jianhong Zhou,<sup>1,\*</sup> Qing Chang,<sup>2</sup> Da Mu,<sup>1</sup> Jinhua Yang,<sup>1</sup> Wenbo Han,<sup>1</sup> Lu Wang<sup>1</sup>

<sup>1</sup>*School of Photoelectric Engineering , Changchun university of science and technology, Changchun, China, 130022*

<sup>2</sup>*College of Electronic Engineering, Heilongjiang University , Harbin 150080*

*\*Corresponding author: zhoujhwd@yahoo.com.cn*

We theoretically investigate the waveguide power splitters with parallel output ports by the time domain coupled-mode theory. Different from the idea of structure with perfect T-type branch and two perfect bends, conditions for perfect transmission and zero reflection are obtained. Using the theoretical analysis, the waveguide power splitters in two-dimensional square lattice photonic crystals are modeled and optimized. Their transmission properties are simulated by using the finite-difference time-domain method, and an excellent agreement has been found with the present analysis.

*OCIS codes:130.2790, 130.1750, 230.7370, 230.1360*

## 1. Introduction

Optical devices based on photonic crystals such as linear waveguide, waveguide bends[1] and waveguide intersections[2], have gained worldwide interest in the past few years due to the advantage of substantial size reduction for the high-density optical integrated circuits. Among the most basic optical devices, waveguide power splitters are key components for the fabrications of Mach-Zehnder interferometers or optical switches, where the two output waveguides are parallel to each other. Many of the power splitters proposed [3-5] are not with the parallel output waveguides and waveguide bends are needed at output ports. While power splitters with the parallel output waveguides based on multimode coupling lead to mode-mixing problems at intersections which results in reflections [6,7]. In this letter, we theoretically investigate the waveguide power splitters with parallel output waveguides by coupled-mode theory and analyze the transmission characteristics of the splitters in two-dimensional square lattice photonic crystals by the finite-difference time-domain method. Different from the idea of splitters with perfect T-type branch and two perfect sharp bends, the conditions for perfect transmission and zero reflection are given.

## 2. Theoretical analysis

Fig. 1 shows the structure of the splitter, which is symmetric with respect to the input waveguide. The connecting waveguide is perpendicular to the input waveguide and the two output waveguides. The junction and the two bends are considered as resonant cavities. The amplitudes of the cavity  $A_1$  and  $A_2$  are denoted by  $a_1$  and  $a_2$  respectively and are normalized to the energy in the modes [8,9]. The amplitudes of the incoming and outgoing waves into the cavity  $A_i$  are denoted by  $S_{+ij}$  and  $S_{-ij}$  ( $i, j = 1, 2$ ) (as shown in Fig. 1) and are also normalized to the power carried by the waveguide mode. The transmission and reflection properties of such a system can be calculated by the coupled-mode theory in time

[8,9]. When the electromagnetic wave at a frequency  $\omega$  is incident upon the system from the input port, i.e.,  $S_{+22} = 0$ , the time evolution of the amplitudes of the cavity  $A_1$  and  $A_2$  in steady state can be described as

$$\frac{da_1}{dt} = j\omega_1 a_1 - \left(\frac{1}{\tau_{11}} + \frac{2}{\tau_{12}}\right)a_1 + (S_{+11}\sqrt{\frac{2}{\tau_{11}}} + 2S_{+12}\sqrt{\frac{2}{\tau_{12}}}), \quad (1)$$

$$\frac{da_2}{dt} = j\omega_2 a_2 - \left(\frac{1}{\tau_{21}} + \frac{1}{\tau_{22}}\right)a_2 + S_{+21}\sqrt{\frac{2}{\tau_{21}}}, \quad (2)$$

where  $\omega_1$  and  $\omega_2$  are the resonant frequencies of cavity  $A_1$  and  $A_2$  respectively,  $1/\tau_{11}$  and  $1/\tau_{12}$  are the decay rates of cavity mode amplitude  $a_1$  into the input waveguide and into the connecting waveguide, and  $1/\tau_{21}$  and  $1/\tau_{22}$  are the decay rates of cavity mode amplitude  $a_2$  into the connecting waveguide and into the output waveguide. From the power conservation and from the time reversal symmetry, the relationships between the amplitudes of the outgoing-incoming waves in the waveguide and the amplitudes of the resonant modes are given by

$$S_{-ij} = -S_{+ij} + \sqrt{\frac{2}{\tau_{ij}}}a_i. \quad (3)$$

Due to the connection of the cavity  $a_1$  and  $a_2$  by waveguides, the incoming waves to the cavities should satisfy the relationships in a steady state:  $S_{-12} = S_{+21} \exp(j\beta d)$  and  $S_{-21} = S_{+12} \exp(j\beta d)$ , where  $\beta$  is the wave propagation constant in the connecting waveguide and  $d$  is the distance from cavity  $A_1$  to cavity  $A_2$ , as shown in Fig. 1. When each of the two bends formed by the connecting waveguide and the output waveguides are symmetry with respect to their own angle bisectors, i.e.,  $1/\tau_{21} = 1/\tau_{22}$ , and when the phase-matching condition

$$\beta d = n\pi \quad (4)$$

is satisfied ( $n$  is an integer), the reflection coefficient  $R$  and the transmission coefficient  $T$  into the output ports can be determined as

$$R = \left| \frac{S_{-11}}{S_{+11}} \right|^2 = \frac{(\omega - \omega_0)^2 + \left( \frac{1}{\tau_1} - \frac{2}{\tau_2} \right)^2}{(\omega - \omega_0)^2 + \left( \frac{1}{\tau_1} + \frac{2}{\tau_2} \right)^2}, \quad (5)$$

$$T = \left| \frac{S_{-22}}{S_{+11}} \right|^2 = \frac{\frac{4}{\tau_1 \tau_2}}{(\omega - \omega_0)^2 + \left( \frac{1}{\tau_1} + \frac{2}{\tau_2} \right)^2}, \quad (6)$$

where

$$\omega_0 = \frac{\tau_{12}\omega_1 + 2\tau_{21}\omega_2}{\tau_{12} + 2\tau_{21}}, \quad (7)$$

$$\frac{1}{\tau_1} = \frac{\tau_{12}}{\tau_{11}} \frac{1}{\tau_{12} + 2\tau_{21}}, \quad (8)$$

$$\frac{1}{\tau_2} = \frac{1}{\tau_{12} + 2\tau_{21}}. \quad (9)$$

Comparing Eq. (5) and Eq. (6) with the results obtained in [3], the splitting region of the input and output waveguides, which consists of three cavities and the connecting waveguides, can be taken as a single mode composite cavity with effective resonant frequency  $\omega_0$ , and the effective decay rates of the composite cavity mode amplitude into the input waveguide and into the output waveguides are  $1/\tau_1$  and  $1/\tau_2$  respectively.

From Eq. (5)-(9), zero reflection can be realized at the frequency  $\omega = \omega_0$ , if the rate-matching condition  $1/\tau_1 = 2/\tau_2$ , *i.e.*

$$\frac{1}{\tau_{11}} = \frac{2}{\tau_{12}} \quad (10)$$

is satisfied, and the power is split equally between the two output ports due to the symmetry of the structure.

For T-type waveguide branch proposed in [3], the resonant frequency and the rate-matching condition are both determined by the branching cavity, whereas for the power splitter with two parallel output waveguides, the effective resonant frequency is determined by the

phase-matching condition described by Eq. (4) and the rate-matching condition is only dependent on the cavity  $A_1$ , which is the same as that of the T-type waveguide branch [3]. So from Eq. (7), we optimize the parameters  $\tau_{21}$  and  $\omega_2$  of the cavity  $A_2$  to make the effective resonant frequency  $\omega_0$  satisfy the phase-matching condition to obtain perfect transmission and zero reflection.

It should be mentioned that when the resonant frequencies of these cavities are the same, the phase-matching condition is not needed any more, which corresponds to the structure with perfect T-type branch and two perfect sharp bends operated at that resonant frequency.

### 3. Design and numerical calculations

Based on the theoretical considerations above, we designed power splitters in a two-dimensional photonic crystal of dielectric rods in air on a square array with lattice constant  $a$ , which possesses a band-gap for transverse magnetic (electric field parallel to the rods) modes[10]. The rods have radius of  $0.20a$  and a dielectric constant of 11.56 (the wavelength dependence of the material refractive indices is ignored). The waveguides are formed by removing rows or columns of rods in the crystal.

In order to study the transmission and reflection properties of the power splitters, the 2D finite-difference time-domain method with perfectly matched layer boundaries [11] is carried out with subpixel smoothing to increase accuracy by using a freely available software package ( Meep ) [12]. The computational cell is shown in the top panel of Fig. 2, where  $d = 3a$ . The simulations are performed at a resolution of  $20 \times 20$  pixels per  $a \times a$ . A dipole located at the entrance of the input waveguide creates a pulse with a Gaussian envelope in time. Two points inside the guides are chosen to monitor the field amplitude, one in the input waveguide (point A) and one in the output waveguide (point B), as indicated in the top panel of Fig.2. By using a sizable computational cell of  $201 \times 25$  lattice constants and by

appropriately positioning the monitor points, we can distinguish and separate all the different pulses propagating in the cell, such as the input pulse, the pulses reflected by and transmitted through the splitter and the pulse reflected from the edges of the crystal. These pulses are shown in the bottom panel of Fig. 2. In our simulation, three pulses covering different ranges of frequencies, as shown in the inset of Fig. 3, are sent down the input waveguide. The input pulses and the pulses transmitted through the splitter are detected by point A and point B respectively, and Fourier transformed to obtain the normalized transmission coefficients for each frequency, as shown in Fig. 3. Although the transmission coefficient remains higher than 45% for a wide range of frequencies between  $0.369(2\pi c/a)$  and  $0.409(2\pi c/a)$ , with a maximum of 48.7% at the frequency  $\omega = 0.392(2\pi c/a)$ , perfect transmission and zero reflection can not be obtained in the whole range of frequencies because the rate-matching condition described by Eq. (10) are not satisfied.

In order to improve the transmission, we satisfy the rate-matching condition that  $1/\tau_{11} = 2/\tau_{12}$  by placing two extra rods with radius  $r = 0.07a$  between the input and the connecting waveguides as done in the literature reported in [3]. Based on the theoretical analysis above, the phase-matching condition described by Eq. (4) is also needed to be satisfied to obtain perfect performance, where only when  $n = 2$  does the effective resonant frequency  $\omega_0$  locate in the photonic band gap. We optimize the parameters  $\tau_{21}$  and  $\omega_2$  to make  $\omega_0$  fit that condition by adjusting the structure of the cavity  $A_2$ . This is achieved by carefully choosing radius  $r_x$  and  $r_c$  of four rods at the bend corners as shown in Fig. 4 (a), where  $r_c = 0.20a$ ,  $r_x = 0.0$ , *i.e.*, cavity  $A_2$  are the structure of sharp bends with zero radius of curvature. Fig. 4 (b) shows the transmission spectra. The transmission coefficient remains higher than 47.5% within a wide frequency ranges between  $0.373(2\pi c/a)$  and  $0.408(2\pi c/a)$ , and the desired 3-dB power splitter operation is obtained at the frequency  $\omega = 0.393(2\pi c/a)$  where the transmission coefficient reaches 50%. The inset of Fig. 4 (b) shows the steady-state field distribution operated at  $\omega = 0.393(2\pi c/a)$  and the input wave splits equally into the two

output waveguides. The performance of the designed splitter is in good agreement with the proposed analysis.

Figure 5(a) shows the another power splitter with  $d = 4a$ , where there are two frequencies located in the photonic band gap met the phase matching condition, *i.e.*,  $n = 2$  or  $n = 3$ . Two extra rods with radius  $0.07a$  are placed between the input and the connecting waveguides to satisfy the rate-matching condition. In order to improve the transmission performance, we need to adjust the effective resonant frequency  $\omega_0$  to satisfy the phase-matching condition. This is achieved by carefully choosing radius  $r_x$  and  $r_c$  of four rods as shown in Fig. 5 (a). The transmission properties are shown in Fig. 5 (b), where the solid line is the transmission spectra for the structure with parameters  $r_c = 0.20a$ ,  $r_x = 0.055a$  and the dash line for the structure with parameters  $r_c = 0.235a$ ,  $r_x = 0.0$ , respectively. For the former structure, the effective resonant frequency  $\omega_0$  is  $0.347(2\pi c/a)$  corresponding to  $n = 2$ , where the transmission reaches maximum 50%. The other transmission peak at  $0.414(2\pi c/a)$  corresponds to the phase matching condition where  $n = 3$ , which is not satisfying the resonant condition. For the latter structure, the transmission coefficient is a slow varying function of the frequency, larger than 45% over a wide range of frequencies between  $0.343(2\pi c/a)$  and  $0.420(2\pi c/a)$ , and reaches maximum at  $\omega_0 = 0.417(2\pi c/a)$  which corresponds to the phase-matching condition where  $n = 3$ .

#### 4. Summary

We have presented a theoretical analysis of waveguide power splitters by the coupled-mode theory. Three conditions for perfect transmission and zero reflection are obtained: rate-matching condition, phase-matching condition and frequency resonant condition. Based on these conditions, numerical simulations of the waveguide power splitters in

two-dimensional photonic crystals with near-complete transmission are demonstrated and an excellent agreement has been found with the present analysis.

### **Acknowledgment**

This work is supported in part by China postdoctoral science project (No.20070410684), Yong science key project of higher institutions of Heilongjiang province (No.1154G25), and science and technology project of education of Heilongjiang province (No.11541265).

### **Reference**

1. A. Mekis, J. C. Chen, I. Kurland, S. Fan, P. R. Villeneuve, J. D. Joannopoulos, "High Transmission through Sharp Bends in Photonic Crystal Waveguides," *Phys. Rev. Lett.*, 77,3787-3790 (1996).
2. S. G. Johson, C. Manolatou, S. Fan, P. R. Villeneuve, J. D. Joannopoulos, H. A. Haus, "Elimination of cross talk in waveguide intersections," *Opt. Lett.* 23, 1855 (1998).
3. S. Fan, S. G. Johnson, J.D. Joannopoulos, "Waveguide branches in photonic crystals," *J. Opt. Soc. Am. B* 18, 162-165 (2001).
4. S. Kim, I. Park, H. Lim, "Proposal for ideal 3-dB splitters-combiners in photonic crystals," *Opt. Lett.* 30, 257-259 (2005).
5. S. Boscolo, M. Midrio, "Y Junctions in photonic crystal channel waveguides: high transmission and impedance matching," *Opt. Lett.* 27, 1001-1003 (2002).
6. T. Liu, A. R. Zakharian, M. Fallahi, M. Mansuripur, "Multimode Interference-based Photonic Crystal Waveguide Power Splitter," *J. Lightwave Techn.*,22, 2842-2846(2004).
7. I. Park, H. -S. Less, H.-J. Kim, K.-M. Moon, S.-G. Lee, B.-H. O, S.-G. Park, E. -H. Lee, "Photonic crystal power-splitter based on directional coupling," *Opt. Exp.*, 12,

3599-3604(2004).

8. H. A. Haus, *Waves and Fields in Optoelectronics* (Prentice-Hall, Englewood Cliffs, N.J., 1984).
9. C. Manolatou, S. G. Johnson, S. Fan, P. R. Villeneuve, H. A. Haus, J. D. Joannopoulos, "High density integrated optics," *IEEE J. of Lightwave Technology*, 17, 1682-1692( 1999).
10. J. D. Joannopoulos, P.R.Villeneuve, and S. Fan, "Photonic crystals: putting a new twist on light," *Nature* 386,143-149 (1999).
11. A. Taflove and S. C. Hagness, *Computational electrodynamics: the finite-difference time-domain method* (Artech House, Norwood, Mass., 2000)
12. A. Farjadpour, D. Roundy, A. Rodriguez, M. Ibanescu, P. Bermel, J. D. Joannopoulos, S. G. Johnson, and G. Burr, "Improving accuracy by subpixel smoothing in FDTD," *Opt. Lett.*, 31, 2972–2974 (2006).

## Figure captions

Fig. 1. Schematic of the theoretical model for waveguide splitter. The black regions represent the waveguides and the white circles represent resonator.

Fig. 2. Top panel: Schematic view of the  $201a \times 25a$  computational cell, where the cavity  $A_1$  is located in the center. The field amplitude is monitored at points A and B, which are placed in the input and output guides of the splitter, respectively. The distance between the two output waveguides is  $6a$ . Bottom panel: Field amplitude recorded at points A and B, as a function of time. The pulses reflected by and transmitted through the splitter, as well as the pulses reflected from the edges of the cell are easily discernible.

Fig. 3. Transmission coefficients for the power splitter shown in the top panel of Fig. 2. The inset is the spectral profile of three input pulses.

Fig. 4. (a) Structure of the power splitter with  $d = 3a$ . (b) Transmission spectra calculated by the finite-different time-domain method. The inset is the electric field distribution at frequency  $\omega_0 = 0.393(2\pi c/a)$ , where red, blue and white represent large positive, large negative and zero fields respectively. The electric field is polarized along the axis of dielectric columns.

Fig. 5. (a) Structure of the power splitter with  $d = 4a$  in two-dimensional photonic crystals made from a square lattice. (b) Transmission spectra calculated by the finite-different time-domain method. Solid line for the structure with  $r_c = 0.20a$ ,  $r_x = 0.055a$ ; Dash line for the structure  $r_c = 0.235a$ ,  $r_x = 0.0$ .

Figure 1 of 5

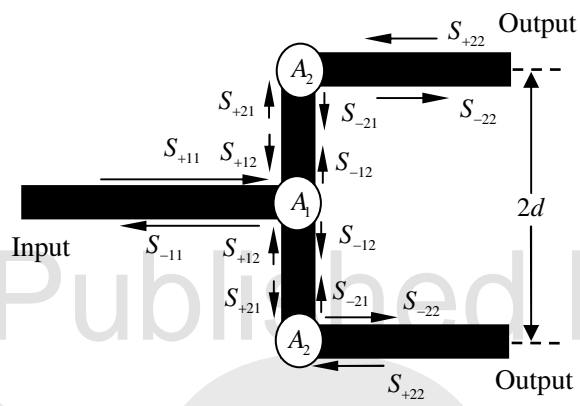


Fig. 1

Figure 2 of 5

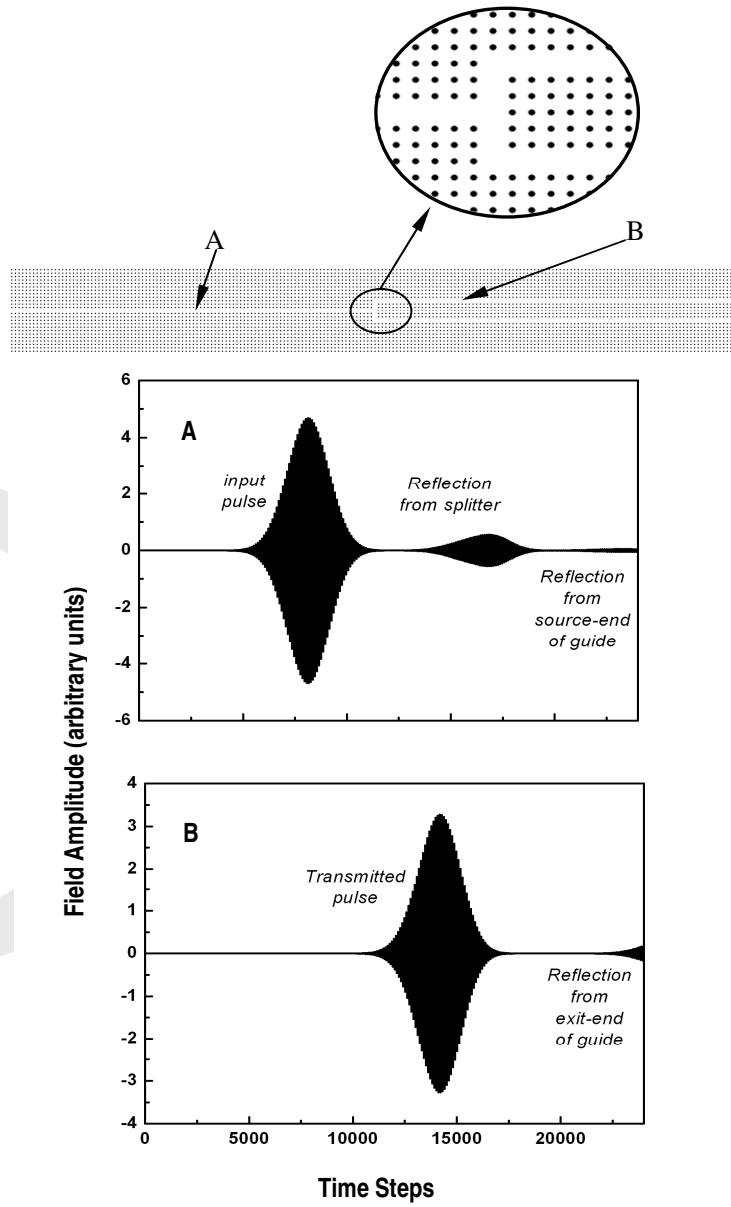


Fig. 2

Figure 3 of 5

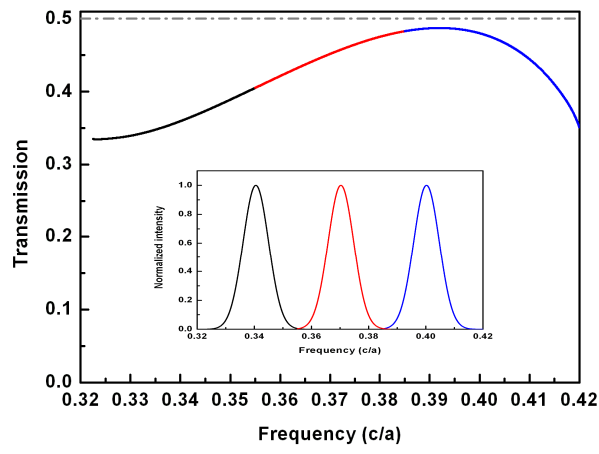


Fig. 3

Figure 4 of 5

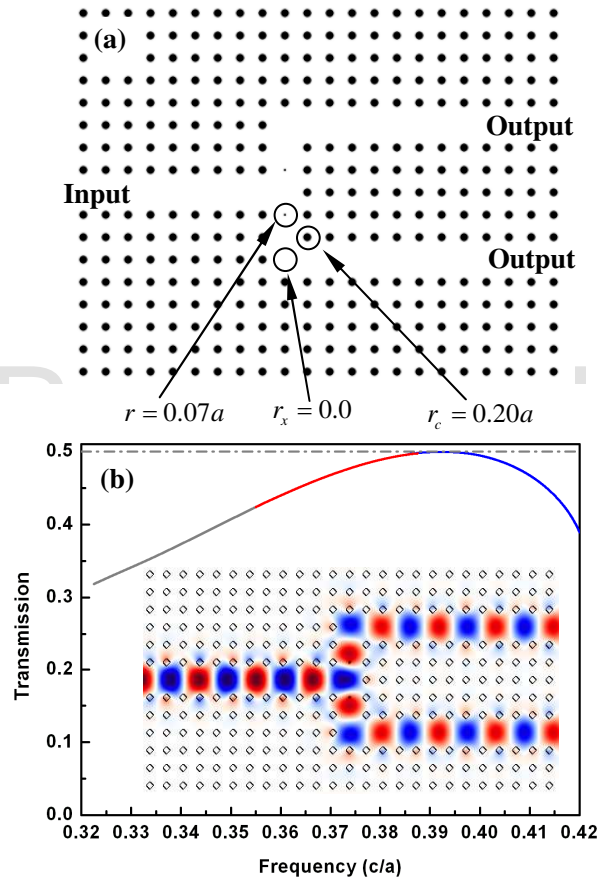


Fig. 4

Figure 5 of 5

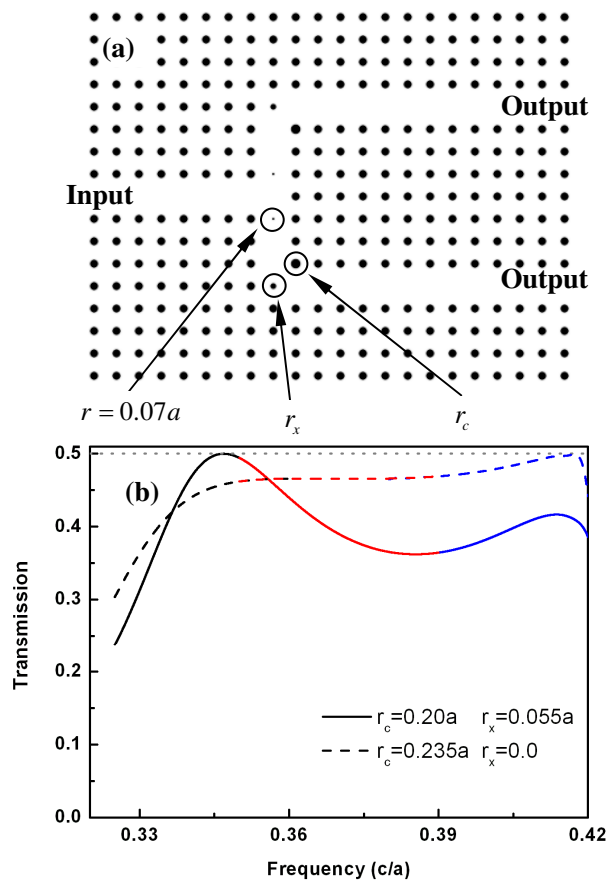


Fig. 5